ORIGINAL ARTICLE

Vascular Endothelial Growth Factor Inhibition by dRK6 Causes Endothelial Apoptosis, Fibrosis, and Inflammation in the Heart via the Akt/eNOS Axis in *db/db* Mice

Cheol Whee Park,[1] Hyung Wook Kim,[1] Ji Hee Lim,[1] Ki Dong Yoo,[1] Sungjin Chung,[1] Seok Joon Shin,[1] Hyun Wha Chung,[1] Sang Ju Lee,[1] Chi-Bom Chae,[2] Yong-Soo Kim,[1] and Yoon Sik Chang[1]

OBJECTIVE—Vascular endothelial growth factor (VEGF), which is associated with the stimulation of angiogenesis and collateral vessel synthase, is one of the crucial factors involved in cardiac remodeling in type 2 diabetes.

RESEARCH DESIGN AND METHODS—We investigated VEGF inhibition by dRK6 on the heart in an animal model of type 2 diabetes. Male *db/db* and *db/m* mice either were treated with dRK6 starting at 7 weeks of age for 12 weeks (*db/db*-dRK6 and *db/m*-dRK6) or were untreated.

RESULTS—Cardiac dysfunction and hypertrophy were noted by echocardiogram and molecular markers in the *db/db*-dRK6 mice. The presence of diabetes significantly suppressed the expression of VEGF receptor (VEGFR)-1 and VEGFR-2, phospho-Akt, and phospho-endothelial nitric oxide synthase (eNOS) in the heart. In *db/db*-dRK6 mice, dRK6 completely inhibited VEGFR-2, phospho-Akt, and phospho-eNOS expression, whereas no effect on VEGFR-1 was observed. Cardiac fibrosis, microvascular scarcity associated with an increase in apoptotic endothelial cells, and inflammation were prominent, as well as increase in antiangiogenic growth factors. Cardiac 8-hydroxy-deoxyguanine and hypoxia-inducible factor-1α expression were significantly increased. No such changes were found in the other groups, including the *db/m*-dRK6 mice. The number of apoptotic human umbilical vein endothelial cells was increased by dRK6 in a dose-dependent manner only at high glucose concentrations, and this was associated with a decrease in phospho-Akt and phospho-eNOS related to oxidative stress.

CONCLUSIONS—Our results demonstrated that systemic blockade of VEGF by dRK6 had deleterious effects on the heart in an animal model of type 2 diabetes; dRK6 induced downregulation of the VEGFR-2 and Akt-eNOS axis and enhancement of oxidative stress. *Diabetes* **58:2666–2676, 2009**

From the [1]Department of Internal Medicine, The Catholic University of Korea, Seoul, Korea; and the [2]Institute of Biomedical Science and Technology, Konkuk University, Seoul, Korea.
Corresponding author: Yoon Sik Chang, ysc543@unitel.co.kr.

Vascular endothelial growth factor (VEGF), especially VEGF-A, is an important mediator of neovascularization, as well as a key factor for maintaining the integrity of endothelial cells in physiologic and pathologic conditions. Two important VEGF receptor tyrosine kinases have been identified and their functions described (VEGF receptor [VEGFR]-1 or Flt-1 and VEGFR-2 or KDR/Flk-1) (1). The deregulation of VEGF results in reduced activation of endothelial nitric oxide synthase (eNOS) and increased production of reactive oxygen species (ROS), which upregulates the expression of procoagulant, prothrombotic, and proinflammatory mediators (2). Several VEGF inhibitors are currently under evaluation or have already been approved for the treatment of age-related macular degeneration and macular edema (3), various cancers (4,5), and diabetic microvascular complications (3). However, there is a growing realization that VEGF inhibitors have significant side effects on the kidney and blood pressure and have been associated with thrombotic microangiopathy, which are typically downstream consequences of suppression of the endothelial Akt-eNOS signaling pathway (4). Impaired cardiac function has been observed in some patients on anti-VEGF therapy (4).

Diabetic cardiomyopathy (DCM) is a clinical condition associated with ventricular dysfunction; DCM develops in patients with diabetes in the absence of atherosclerosis and hypertension (6–9). Left ventricular diastolic and systolic dysfunction and alterations in the coronary microcirculation, as well as interstitial fibrosis, are characteristics of DCM because of a reduced microvasculature (10–12). There continues to be debate about the role of VEGF with regard to the heart in diabetic patients. Expression of VEGF and VEGFR-2 in the human heart, and in streptozotocin-induced diabetic animals, has been shown to be significantly decreased because of loss of insulin-induced VEGFR-eNOS axis activation (13–15), which is followed by an increase of apoptosis in endothelial cells, a decrease in the number of circulating endothelial progenitor cells, decreased capillary density, and impaired myocardial perfusion (14–16). Downregulation of VEGF in the heart is associated with an increased risk for cardiovascular morbidity and mortality in diabetic patients (16). Both increased and unaltered serum or plasma VEGF levels were observed in type 1 and 2 diabetic patients versus control subjects (17,18). On the other hand, the serum VEGF level is increased in patients with diabetic symptomatic poly-

neuropathy, overt diabetic nephropathy, and coronary artery disease, particularly related to the extent of myocardial damage (19–21).

dRK6 is an arginine-rich anti-VEGF hexapeptide and a d-amino acid derivative of RK6 (Arg-Arg-Lys-Arg-Arg-Arg). dRK6 binds with VEGF-A and can thereby block the interaction between VEGF-A (mainly $VEGF_{165}$ and $VEGF_{121}$) and the VEGFRs. In a previous study, dRK6 showed significant inhibition of VEGF-induced angiogenesis and retarded the growth and metastasis of colon carcinoma cells without direct cytotoxicity (22). dRK6 is stable, and its half-life at 37°C in the serum is 13.5 h (22). Previous results demonstrated that a subcutaneous injection of dRK6 (25–50 μg) every other day for 3 weeks reduced the incidence and severity of collagen-induced arthritis in a dose-dependent manner without any toxicity (22,23).

Therefore, we determined whether systemic VEGF blockade, using dRK6, could lead to structural and functional deterioration of the heart in *db/db* mice in a murine model of type 2 diabetes.

RESEARCH DESIGN AND METHODS

Experimental methods. All experiments were performed according to the institutional animal care guidelines, and the investigation conformed with the *Guide for the Care and Use of Laboratory Animals* published by the U.S. Institutes of Health (National Institutes of Health Publication No. 85–23, revised 1996). Six-week-old male C57BLKS/J *db/db* and *db/m* mice were purchased from Jackson Laboratories (Bar Harbor, ME); *db/m* mice were used as controls in all of the experiments. Fifty micrograms of dRK6 was administered three times per week by intraperitoneal injection to *db/m* (*db/m*-dRK6) or *db/db* (*db/db*-dRK6) mice (*n* = 8) beginning at 7 weeks of age for 12 weeks (*n* = 8). The diabetic *db/db* (*db/db*) and nondiabetic *db/m* control groups (*db/m*) received only PBS.

After 12 weeks of treatment, the systolic blood pressure was determined by the noninvasive tail cuff system in conscious mice (IITC Life Science, Woodland Hill, CA) after a 5-day accommodation. At the end of the study, the animals were anesthetized and killed.

Measurement of serum parameters. Blood was collected from the left ventricle and centrifuged; the plasma was stored at −70°C for subsequent analyses. The A1C was measured by high-pressure liquid chromatography (BioRad, Richmond, CA). The total cholesterol, triglycerides, free fatty acids (FFAs), and insulin concentrations were measured by an autoanalyzer (Wako, Osaka, Japan). We also measured the serum VEGF concentration using an ELISA kit (Komabiotech, Seoul, South Korea).

Assessment of heart function. During the last week of the study, we performed an echocardiogram to evaluate the heart function and size in the animals using a Hewlett-Packard Sonus 4500 ultrasound machine (Agilent Technologies, Edmonton, AB, Canada) while the animals were anesthetized according to a procedure previously reported (24).

Light microscopy. The heart samples were collected after systemic perfusion with PBS and then fixed in 4% paraformaldehyde. To examine the effect of dRK6 on cardiac fibrosis, the analysis was performed on trichrome-stained heart sections as described previously (25). Ten consecutive heart cross-sections were photographed by an examiner who was blinded to the source of the tissue using a digital camera (Olympus DP11; Olympus America, Melville, NY).

Immunohistochemistry for connective tissue growth factor, platelet-endothelial cell adhesion molecule-1, thrombospondin-1, transferase-mediated dUTP nick-end labeling, F4/80, and 8-hyrdoxy-deoxyguanosine (8-OH-dG). We performed immunohistochemistry for connective tissue growth factor (CTGF), F4/80, platelet-endothelial cell adhesion molecule (PECAM)-1, thrombospondin-1, transferase-mediated dUTP nick-end labeling (TUNEL), and 8-hyrdoxy-deoxyguanosine (8-OH-dG). Five-μm thick sections were incubated overnight with anti-CTGF as a profibrotic growth factor (1:250 in blocking solution; Abcam, Cambridge, U.K.), anti–PECAM-1 as a mouse endothelial cell marker (1:50; BD Bioscience, San Diego, CA), antithrombospondin-1 as an antiendothelial cell growth factor (1:100; Lab Vision, Fremont, CA), the in situ TUNEL assay as an apoptotic marker (Apoptag Plus, Intergen, New York, NY), anti-F4/80 as an inflammatory cell marker (1:50; Serotek, Oxford, U.K.), and 8-OH-dG as a marker of oxidative DNA damage (1:100; JalCA, Shizuoka, Japan) in a humidified chamber at 4°C. Antibodies were localized with the ABC technique (Vector, Buringame, CA). We also measured 8-OH-dG levels from the purified DNA of the hearts performed with an ELISA kit.

For the quantification of the proportions of the areas stained, ~20 views were randomly located in the middle portion of the myocardium of each slide (Scion Image Beta 4.0.2; Frederick, MD). The endothelial cells that were positive for apoptosis exhibited an intense brown nuclear (TUNEL-positive) and a red cytoplasmic colorimetric (PECAM-1–positive) reaction product. The number of cells positive for the TUNEL reaction was determined in the myocardium under ×400 magnification.

Immunofluorescent staining for the hypoxia-inducible factor-1α. To evaluate the hypoxic injury to the heart, we performed hypoxia-inducible factor (HIF)-1α immunofluorescent staining of the heart (1:50; Novous Biological, Littleton, CO). For quantification of the proportion of the area stained, ~20 views (×200 magnification), randomly located in the middle portion of the myocardium of each slide, were also examined (Scion Image Beta 4.0.2).

Western blot and semi-quantitative RT-PCR for total- and phospho-eNOS (Ser^{1177}), total- and phospho-Akt (Ser^{473}), VEGFR-1, VEGFR-2, CTGF, and HIF-1α. Western blot analysis was performed using the following antibodies: total Akt, phospho-Akt (Ser^{473}), total eNOS, and phospho-eNOS (Ser^{1177}; all from Cell Signaling Technology, Danvers, MA) and HIF-1α, CTGF, and β-actin (all from Abcam, Cambridge, U.K.). Protein for HIF-1α from nuclear fractions of the hearts was isolated using a nuclear extraction kit (Cayman Chemical, Ann Arbor, MI) following the manufacturer's protocol. We also performed RT-PCR to assess the levels of gene expression of VEGFR-1 and -2, HIF-1α, CTGF, and 18r rRNA as an internal control. Primers for amplification of VEGFR-1 and -2, HIF-1α, CTGF, and 18r rRNA are listed in the supplemental data available in an online appendix at http://diabetes.diabetesjournals.org/cgi/content/full/db09-0136/DC1.

Quantitative PCR for atrial natriuretic factor, B-type natriuretic peptide, α-myosin heavy chain, and β-myosin heavy chain. Total reactive nitrogen species was performed using an ABI PRISM Sequence Detector System 7500 (Applied Biosystems, Foster City, CA). The PCR primers for atrial natriuretic factor (ANF), B-type natriuretic peptide (BNP), α-myosin heavy chain (MHC), and β-MHC are listed in the supplemental data.

TUNEL assay, 8-iso-$PGF_{2\alpha}$ and 8-OH-dG levels in the human umbilical vein endothelial cell culture. Human umbilical vein endothelial cells (HUVECs) were cultured in RPMI 1640 supplemented with 10% FBS and 15 mg/500 ml of endothelial cell growth supplement (Sigma, St. Louis, MO) at 37°C in a humidified, 5% CO_2/95% air atmosphere. Apoptosis was quantified with the in situ cell death detection kit, using a TUNEL assay (Chemicon International, Temecula, CA). After treatment with different concentrations of D-glucose in the media (5 and 30 mmol/l per liter of D-glucose and D-glucose [5 mmol/l per liter] + D-mannitol [25 mmol/l per liter]) with 0, 10^{-6}, 10^{-8}, or 10^{-10} mmol/l dRK6 for 48 h, the number of TUNEL-positive cells was counted in 10 randomly chosen fields at a magnification of ×400. We also performed Western blot analysis using 10^{-8} mmol/l dRK6 for 48 h with the following antibodies: total Akt, phospho-Akt (Ser^{473}), total eNOS, and phospho-eNOS (Ser^{1177}). To evaluate the direct effects of dRK6 on oxidative stress, we also measured the concentrations of 8-iso-$PGF_{2\alpha}$ and 8-OH-dG in the cell culture media.

Statistical analysis. Data are expressed as the means ± SD. The differences between the groups were examined for statistical significance using ANOVA with the Bonferroni's correction (SPSS 11.5; Chicago, IL). Nonnormally distributed data were analyzed by the nonparametric unpaired Mann-Whitney *U* test. A *P* value ≤0.05 was considered a statistically significant difference.

RESULTS

Body weight, heart weight, mean systolic blood pressure, and the hematocrit. The body weights of the *db/db* mice with or without dRK6 treatment were heavier than the *db/m* mice at the end of the experiment (*P* < 0.01, Table 1). There was a slightly heavier heart weight in the *db/db*-dRK6 group compared with the other groups, but the difference was not statistically significant. There was no significant difference in mean systolic blood pressure (SBP) between the *db/m* and *db/db* mice with or without dRK6 treatment.

Fasting blood glucose, A1C, serum lipids, insulin levels, and serum VEGF. As expected, there were significant increases in the fasting blood glucose (FBG) and A1C, total cholesterol, triglycerides, FFAs, and insulin concentrations in the *db/db* and *db/db*-dRK6 mice compared with the *db/m* and *db/m*-dRK6 mice (*P* < 0.05, *P* < 0.01, or *P* < 0.001, respectively; Table 1). By contrast, there was no such difference observed between the *db/db* mice and *db/db*-dRK6 mice. There were significant increases in

TABLE 1
Influence of dRK6 on physiologic and biochemical parameters and serum lipid profiles in *db/db* and *db/m* mice

	db/m	*db/m*-RK6	*db/db*	*db/db*-RK6
Body weight (g)	31.6 ± 1.2	31.2 ± 1.3	50.3 ± 5.8*	42.4 ± 5.9*
Heart weight (g)	0.12 ± 0.04	0.11 ± 0.05	0.12 ± 0.04	0.14 ± 0.05
Mean SBP (mmHg)	95.6 ± 5.4	97.6 ± 3.5	99.1 ± 6.2	102.3 ± 5.0
Hematocrit (%)	34.0 ± 2.9	35.6 ± 3.4	39.8 ± 5.2	38.6 ± 6.4
Glucose (mmol/l)	11.2 ± 1.1	11.8 ± 1.9	58.0 ± 5.9†	57.6 ± 7.8†
A1C (%)	4.3 ± 0.2	4.1 ± 0.3	12.7 ± 1.2†	13.6 ± 1.0†
Total cholesterol (mmol/l)	1.66 ± 0.38	1.53 ± 0.34	2.08 ± 0.37	1.92 ± 0.31
Triglycerides (mg/dl)	60 ± 16	66 ± 20	103 ± 27‡	114 ± 21‡
FFAs (mEq/l)	1.45 ± 0.34	1.57 ± 0.55	3.18 ± 1.03‡	3.76 ± 1.19‡
Insulin (pg/ml)	0.17 ± 0.13	0.19 ± 0.14	0.50 ± 0.14‡	0.33 ± 0.21‡
Serum VEGF (pg/ml)	1.25 ± 1.73	23.5 ± 7.7§	6.6 ± 3.9‡	29.6 ± 8.5§

Data are means ± SD. *$P < 0.01$, †$P < 0.001$, ‡$P < 0.05$ vs. *dm* and *dm-dRK6*. §$P < 0.001$ vs. *dm* and $P < 0.05$ vs. *db/db*.

the serum VEGF concentrations in the *db/m*-dRK6 and the *db/db*-dRK6 mice compared with the *db/m* and *db/db* control mice ($P < 0.001$ and $P < 0.05$, respectively). These findings suggest that VEGF blockade with dRK6 significantly increased the circulating VEGF concentrations.

Assessment of heart function. To assess heart function, we performed echocardiograms on the mice in the study groups (Fig. 1*A*). There were no significant differences in the diastolic interventricular wall thickness (IVSTd), left ventricular posterior wall thickness (LVPWTd), and left ventricular mass (LVM) among the *db/m*, *db/m*-dRK6, and *db/db* mice. By contrast, these parameters in the *db/db*-dRK6 mice were markedly increased compared with the other groups ($P < 0.05$, Fig. 1*B*). Molecular markers of cardiac hypertrophy (ANF, BNP, α-MHC, and β-MHC) were also elevated in the *db/db*-dRK6 mice ($P < 0.05$, Fig. 1*D*). These results suggest that dRK6 treatment caused development of cardiac hypertrophy. Diabetic *db/db* mice also exhibited a persistent decrease in fractional shortening ($P < 0.05$, Fig. 1*C*) compared with the *db/m* mice. There was a more prominent decrease in the fractional shortening, mean velocity of circumferential fiber shortening (Vcf), and peak E/A ratio in the *db/db*-dRK6 mice. These findings demonstrate that treatment with dRK6 had a negative effect on the cardiac function in the presence of diabetes.

Effect of dRK6 on VEGFR-1 and -2, Akt, and eNOS on the heart. As shown in Fig. 2*A*–*C*, there were marked decreases in the expression of VEGFR-1 and -2 mRNA in the *db/db* control mice compared with the *db/m* mice. In addition, dRK6 treatment completely abolished the expression of VEGFR-2 mRNA and protein in *db/db*-dRK6 mice. By contrast, there was no change in the expression of VEGFR-1 mRNA in *db/db*-dRK6 mice; no such changes were detected in *db/m*-dRK6 mice. There was significantly decreased expression of phospho-Akt protein, eNOS mRNA, and phospho-eNOS protein in *db/db* mice compared with *db/m* mice (Fig. 2*D*–*G*). Consistent with the VEGFR-2 findings, dRK6 treatment completely inhibited expression of phospho-Akt/eNOS protein in *db/db*-dRK6 mice.
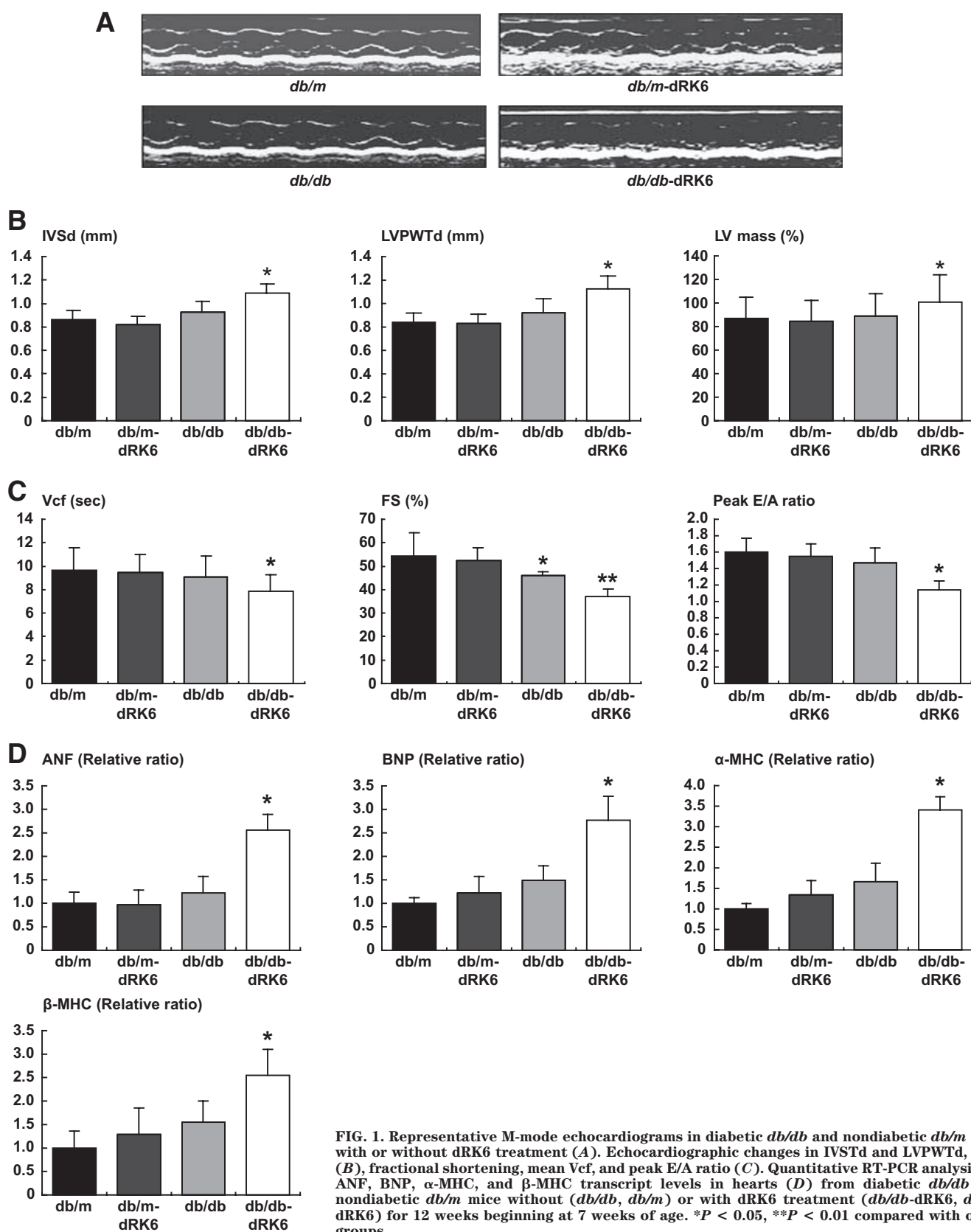
Histologic examination of the heart and effects on connective tissue growth factor. In the *db/m* and *db/db* control mice, there was no apparent cardiac fibrosis observed, which was likely because of the short period of diabetes exposure (Fig. 3*A* and *B*). However, dRK6 treatment markedly increased the cardiac fibrosis observed in the *db/db*-dRK6 mice ($P < 0.05$, Fig. 3*D* and *E*). By contrast, there was no such change observed in the *db/m*-dRK6 mice (Fig. 3*B*). We also performed immunostaining, Western blot, and RT-PCR for CTGF to evaluate the expression of profibrotic and inflammatory growth factors in the heart. Compared with the increased myocardial fibrosis in the heart, the positive staining for CTGF was significantly increased in the *db/db*-dRK6 mice compared with the *db/db* and *db/m*-dRK6 mice ($P < 0.05$, Fig. 4*A*–*E*). Consistent with the immunostaining results, the expression of CTGF mRNA and protein levels was also significantly increased in the *db/db*-dRK6 mice (Fig. 4*F* and *G*). These findings suggest that CTGF is one of the major profibrotic growth factors in dRK6-induced cardiac fibrosis.

Immunohistochemistry for PECAM-1, TUNEL, thrombospondin-1, and F4/80. To evaluate vascular homeostasis, we performed immunohistochemistry staining for PECAM-1, PECAM-1+TUNEL, and thrombospondin-1. There were no changes in the expression of PECAM-1 in *db/db* mice. By contrast, dRK6 treatment in *db/db*-dRK6 mice was associated with a decrease in expression of PECAM-1 in the myocardium, reflecting a decrease in endothelial cells (Fig. 5*A*–*E*). It is well known that thrombospondin-1 is an antiangiogenic peptide; therefore, we evaluated the expression of thrombospondin–1 in the heart. The expression of thrombospondin-1 was significantly increased in the *db/db*-dRK6 mice compared with the *db/m*, *db/m*-dRK6, and *db/db* mice ($P < 0.05$, Fig. 5*F*–*J*). Further evaluation of the effects of endothelial cell apoptosis on the rare vessels in the heart was assessed by double immunostaining with PECAM-1+TUNEL in the heart. It was difficult to find TUNEL-positive stained endothelial cells in the *db/m*, *db/m*-dRK6, and *db/db* mice. By contrast, an increased number of TUNEL-positive cells were found in the *db/db*-dRK6 mice ($P < 0.001$, Fig. 5*K*–*O*).

Only mild macrophage infiltration, as assessed by F4/80-positive staining, was observed in the myocardium of *db/mb*-dRK6 and *db/db* mice. By contrast, F4/80 immunostaining was markedly increased in the myocardium of *db/db*-dRK6 mice ($P < 0.001$, Fig. 4*P*–*T*).

Effect of dRK6 on HIF-1α and 8-OH-dG. There was no difference in expression of HIF-1α in the hearts of *db/m*, *db/m*-dRK6, and *db/db* mice. However, in *db/db*-dRK6 mice, expression of HIF-1α was significantly increased compared with the other groups ($P < 0.001$, Fig. 6*A*–*E*). The expression of HIF-1α protein and mRNA levels in the heart significantly increased in *db/db*-dRK6 mice (Fig. 6*F*–*H*). Diabetic *db/db* mice and *db/m*-dRK6 mice had increased immunostaining of 8-OH-dG in the myocardial cells compared with *db/m* mice (Fig. 6*I*). In the myocardium, increased expression of 8-OH-dG (dark brown nucleus) in *db/db* mice was markedly accentuated by treatment with dRK6 (Fig. 6*L* and *M*). The 8-OH-dG levels

FIG. 1. Representative M-mode echocardiograms in diabetic *db/db* and nondiabetic *db/m* mice with or without dRK6 treatment (*A*). Echocardiographic changes in IVSTd and LVPWTd, LVM (*B*), fractional shortening, mean Vcf, and peak E/A ratio (*C*). Quantitative RT-PCR analysis for ANF, BNP, α-MHC, and β-MHC transcript levels in hearts (*D*) from diabetic *db/db* and nondiabetic *db/m* mice without (*db/db*, *db/m*) or with dRK6 treatment (*db/db*-dRK6, *db/m*-dRK6) for 12 weeks beginning at 7 weeks of age. *$P < 0.05$, **$P < 0.01$ compared with other groups.

in the DNA from the hearts were significantly increased compared with *db/db* mice (Fig. 6*M*), the levels of which were also increased compared with *db/m* mice. These findings suggest that dRK6 treatment increased oxidative stress in the hearts, especially in mice with diabetes.

Effect of dRK6 on HUVEC apoptosis. To examine the direct role of dRK6 on HUVECs, we investigated whether dRK6 induced apoptosis of the HUVECs using TUNEL assay with different doses of dRK6 (10^{-6}, 10^{-8}, and 10^{-10} mmol/l) and various concentrations of glucose in the
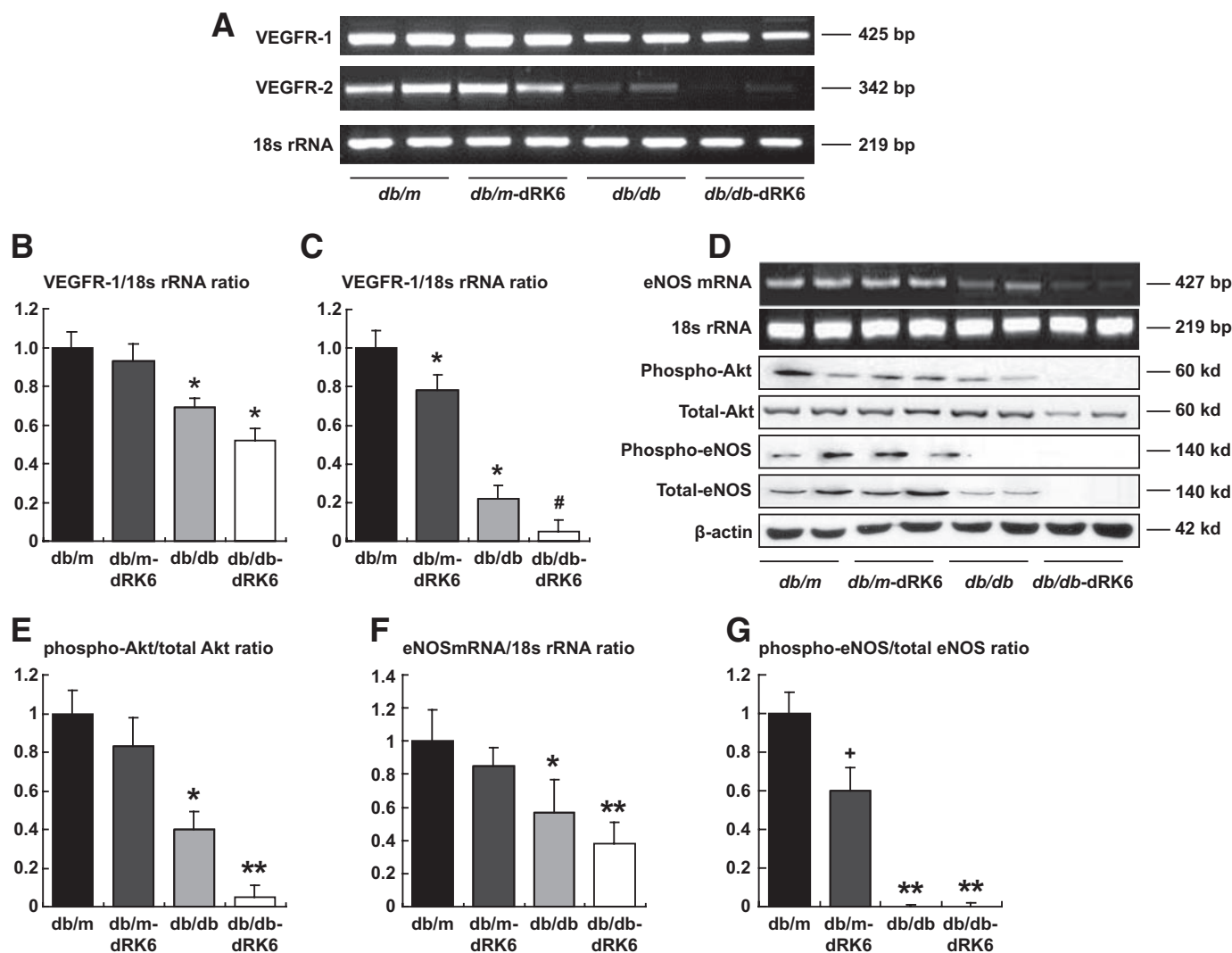
FIG. 2. RT-PCR for VEGF-R1, VEGF-R2 (*A*), eNOS (*D*) mRNA, and 18s rRNA expression in the hearts of diabetic *db/db* and nondiabetic *db/m* mice with or without dRK6 treatment. Quantitative assessment of the expression of VEGF-R1 (*B*), VEGF-R2 mRNA (*C*), and eNOS mRNA (*F*) to 18s rRNA ratios in the hearts of the study groups. Western blot analysis of the total and phospho-Akt and phospho-eNOS (*D*) and quantitative assessment of the expression of total and phospho-Akt (*E*) and phospho-eNOS protein (*G*). *$P < 0.05$ compared with other groups, **$P < 0.01$ compared with other groups, #$P < 0.05$ compared with the *db/db* group, +$P < 0.05$ compared with the *db/m* group; $n = 4$.

media (5 and 30 mmol/l of D-glucose, and 5 mmol/l D-glucose + 25 mmol/l mannitol) for 48 h. Only at a concentration of 30 mmol/l of D-glucose were the HUVEC TUNEL-positive cells significantly increased in a dose-dependent manner ($P < 0.01$, Fig. 7). Treatment with dRK6 completely inhibited the expression of phospho-Akt and phospho-eNOS protein with high glucose concentrations in the media (Fig. 7*B*). However, there was no significant difference in phospho-Akt and phospho-eNOS protein expression for concentrations of 5 mmol/l D-glucose or 5 mmol/l D-glucose + 25 mmol/l mannitol treated with or without dRK6. As shown in Fig. 6*F* and *G*, the 8-iso-PGF$_{2\alpha}$ and 8-OH-dG concentrations were increased with high glucose concentrations, which were further increased by dRK6 treatment (3.0- and 3.5-fold, respectively). However, these changes were not observed at concentrations of 5 mmol/l D-glucose (low glucose) or 5 mmol/l D-glucose + 25 mmol/l mannitol.

DISCUSSION

A growing number of drugs that inhibit VEGF signaling are being considered for the treatment of cancer and diabetic microvascular complications. These agents are generally well tolerated but sometimes may be accompanied by serious side effects. Most of the side effects are associated with downstream effects of suppression of VEGF-NO signaling through the inhibition of VEGF-A and VEGFR-2 signals in the endothelial cells of normal organs (4). Therefore, we evaluated the role of VEGF inhibition using dRK6 in the development and progression of cardiac adverse effects in a model of type 2 diabetes (*db/db* mice). In *db/db* mice, systemic dRK6 administration completely inhibited the cardiac VEGFR-2–Akt-eNOS axis, which subsequently caused the development of systolic dysfunction, cardiac fibrosis, and hypertrophy. From one perspective, the deterioration caused by dRK6 might be related to the regression of blood vessels, which was associated with an increase in antiangiogenic growth factors, such as thrombospondin-1, transforming growth factor (TGF)-β, and CTGF. These events were accompanied by an increase in endothelial cell apoptosis, inflammatory cell infiltration, and myocardial fibrosis. In addition, these pathologic alterations led to the aggravation of hypoxic and oxidative stress in the myocardium accompanied by metabolic ab-
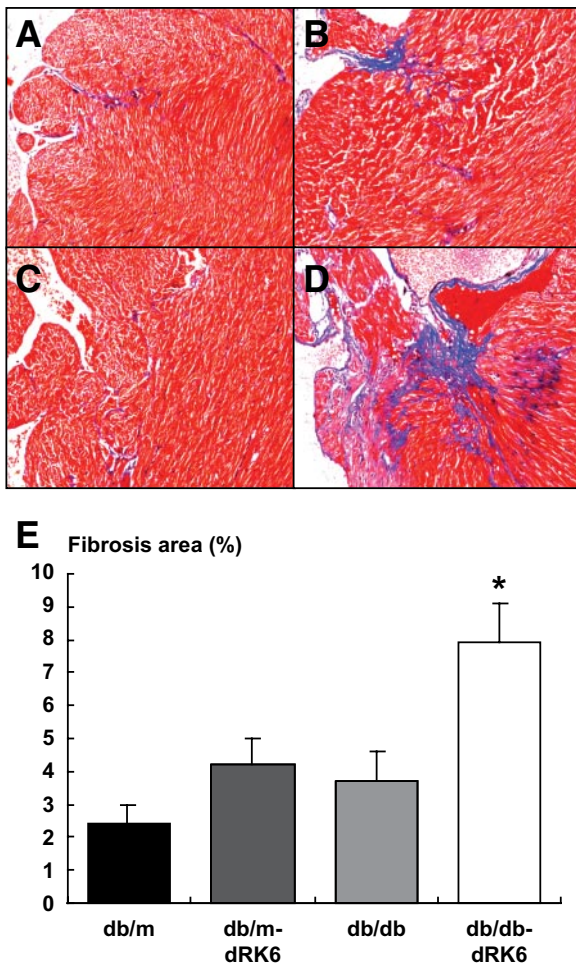
FIG. 3. Cardiac histopathology in diabetic *db/db* and nondiabetic *db/m* mice with or without dRK6 treatment (Trichrome stain, ×100). The histopathology shows marked cardiac fibrosis in diabetic *db/db*-dRK6 (*D*) compared with nondiabetic *db/m* and *db/m*-dRK6 mice (*A* and *B*) and *db/db* control mice (*C*). Original magnification ×200. Quantitative assessment of the areas of fibrosis in the myocardial tissue of the study groups (*E*). *$P < 0.01$ compared with the other groups; $n = 4$. (A high-quality color digital representation of this figure is available in the online issue.)

normalities. However, no such changes were observed in the diabetic control or *db/m*-dRK6 mice. By using in vitro HUVECs, we have shown that dRK6 had potent apoptotic effects on endothelial cells, which were associated with inhibition of the phospho–Akt-eNOS axis and enhancement of oxidative stress.

To date, the effects of systemic inhibition of VEGF on the heart remain uncertain. Previous findings from studies of the structural and functional changes in the organs of the normal adult mouse, after inhibition of VEGF signaling, revealed little or no capillary regression was detected in the brain, retina, skeletal muscle, lung, or myocardium (26,27). Consistent with these findings, our study also demonstrated that there was no change in the microvasculature in the heart of nondiabetic *db/m* mice. However, there was significant regression of the microvasculature of the heart in the diabetic mice, which resulted in cardiac fibrosis and cardiac dysfunction. These findings suggest that diabetes may be a critical determinant of the adverse effects on the heart caused by systemic anti-VEGF therapy.

It has been shown that downregulation of expression of myocardial VEGF and VEGFR-1 and -2 preceded all other characteristic features of DCM (10). These findings suggest that downregulation of VEGF and VEGFR-2 is involved in the microvascular homeostasis of the myocardium and thereby play a central role in the pathogenesis of DCM. In addition, continuous and prolonged VEGF blockade caused by deterioration of the DCM in mice with type 2 diabetes appears to relate to the downregulation of the VEGFR-2–Akt-eNOS axis. The relationship between VEGF expression, the microvasculature, and cardiac function has been clearly demonstrated in experiments on transgenic mice lacking VEGF isoforms, VEGF164 and VEGF188. These mice exhibit impaired myocardial angiogenesis and subsequently developed severe left ventricular dysfunction (28,29). There is growing evidence from animal models and patient studies that DCM can result from microcirculatory defects in the absence of epicardial coronary artery stenosis (30). These findings suggest that decreased VEGF expression might play a significant role in the development of microvascular defects, ischemia, and fibrosis in the pathogenesis of DCM (13).

An important question with regard to VEGF blockade is whether its effects on the heart are through metabolic abnormalities and/or whether there is a direct effect of VEGF on the cardiac microvasculature. Continuous damage to endothelial cells by metabolic abnormalities, including hyperglycemia, advanced glycosylation end products, and FFAs, ultimately leads to cell loss, reduced blood flow, hypoxia, and tissue ischemia (31,32). The results of our in vitro study suggest that metabolic abnormalities, especially hyperglycemia, have deleterious effects on the heart related to VEGF blockade.

It is well known that hypoxia plays a key role in all diabetes-related complications (33). Hyperglycemia-induced oxidative stress is a major risk factor for the development of microvascular pathology in the diabetic myocardium and results in myocardial cell death, hypertrophy, fibrosis, endothelial dysfunction, and even death via the phosphatidylinositol 3-kinase and Akt signaling pathways (34,35). Numerous studies have shown that Akt promotes cardioprotection and inhibits cell apoptosis by regulation of multiple substrates (36,37). Akt phosphorylates and inactivates proapoptotic proteins including glycogen synthase kinase-3β and caspase-9, the upstream activator of caspase-3 (38,39). Akt also activates the antiapoptotic Bcl-2 protein, which is associated with phosphorylation of NOS and increases in the production of NO. Therefore, downregulation of the Akt-eNOS axis by dRK6 might relate to endothelial cell apoptosis in diabetic *db/db* mice.

Under hypoxic conditions, HIF-1α is stabilized, translocates into the nucleus, dimerizes with HIF-1β, and upregulates the genes involved in angiogenesis, glycolytic energy metabolism, cell proliferation, and survival (40,41). In the present study, the markedly upregulated expression of nuclear HIF-1α after treatment with dRK6 suggests that the dRK6-induced hypoxic conditions in the heart and HIF-1α function to prevent excessive ROS production under conditions of chronic hypoxia. These results indicate that continuous VEGF blockade by dRK6 under diabetic conditions ultimately leads to the accumulation of reactive oxygen species and oxidative stress leading to increased expression of 8-OH-dG in the heart.

Previous reports have demonstrated that *db/db* mice usually have no gross cardiac hypertrophy at 3 months (42,43); isolated working hearts as well as studies using magnetic resonance imaging, however, indicate that significant left ventricular dysfunction develops in the hearts
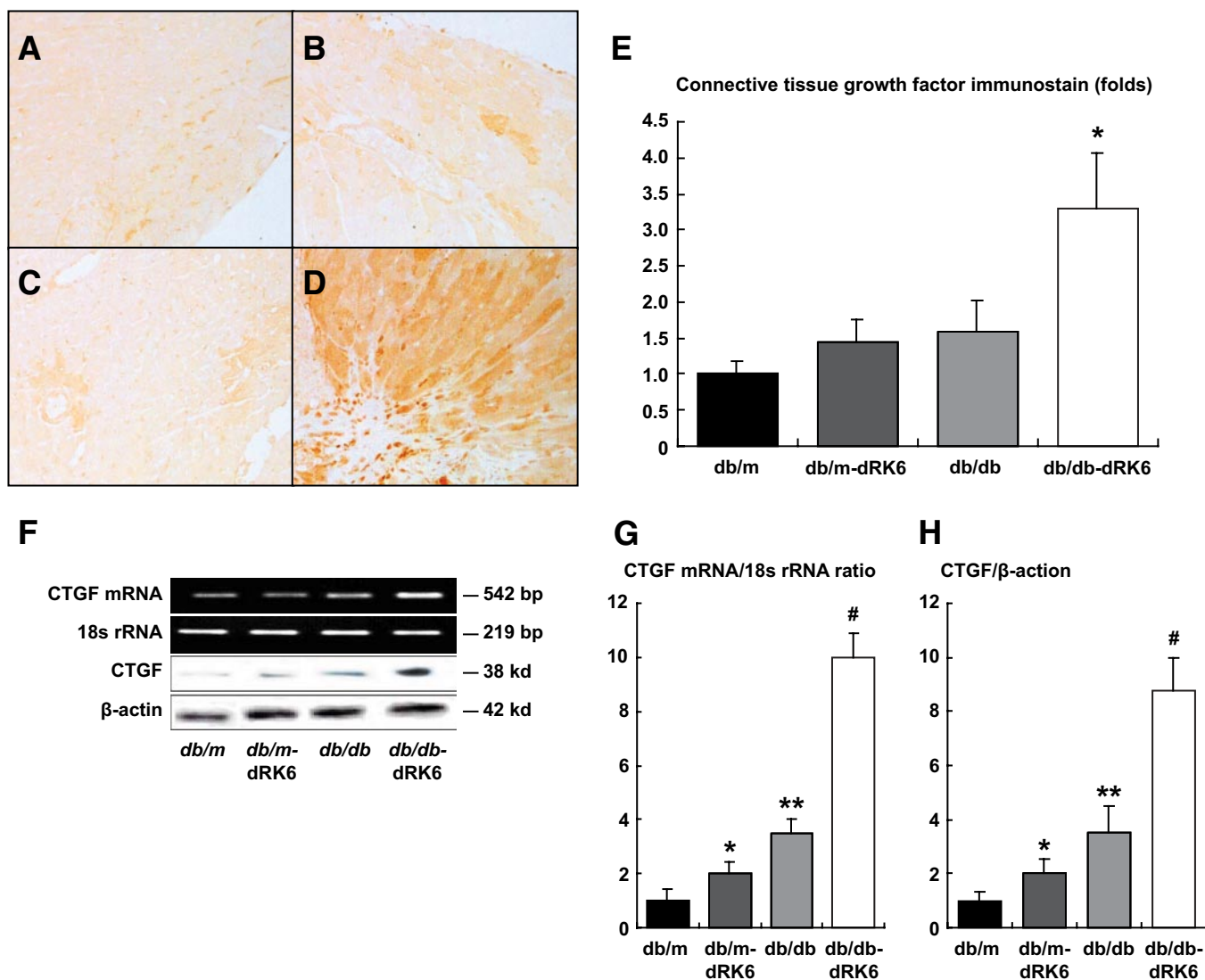
FIG. 4. Immunohistochemical staining for CTGF in the myocardial tissue of nondiabetic *db/m* and diabetic *db/db* mice (*B* and *D*, respectively) with or without dRK6 treatment (*A* and *C*, respectively; ×200). Original magnification ×200. *E*: Quantitative assessment of CTGF immunostaining in the myocardial tissue of the study groups. *F*: Expression of CTGF protein, mRNA, and 18s rRNA in the hearts of the study groups. Quantitative assessment of the expression of CTGF mRNA (*G*) and protein (*H*). *P < 0.05, **P < 0.01 compared with the other groups, #P < 0.01 compared with the *db/db* group; n = 4. (A high-quality color digital representation of this figure is available in the online issue.)

of *db/db* mice at much earlier ages. In this study, in contrast to the *db/db* control mice, systemic inhibition with dRK6 resulted in more severe systolic dysfunction and gross cardiac hypertrophy and fibrosis in the *db/db* mice at 5 months of age. The data from our study showed that the direct effects of VEGF blockade, as well as the metabolic abnormalities associated with diabetes such as hyperglycemia, dyslipidemia, and hyperinsulinemia, might be important to the development of pathologic conditions, including severe cardiac hypertrophy, fibrosis, and inflammation.

Data regarding circulating VEGF levels in diabetes are highly discrepant. One study reported that plasma VEGF levels were higher in type 2 diabetics that in controls (20). In another study, plasma VEGF levels were elevated only in type 2 diabetic patients with characteristics of atherosclerosis (21). In our study, there were sixfold higher serum VEGF levels in *db/db* mice compared with *db/m* mice. dRK6 treatment also increased the serum VEGF level independently from diabetic conditions. It is well known that as VEGF is a paracrine mediator, systemic levels may not adequately reflect changes in the local

VEGF system (44). Therefore, elevated plasma VEGF levels after dRK6 treatment might be a consequence of feedback of systemic VEGF-VEGFR inhibition.

In summary, our results indicate that the systemic dRK6 completely inhibited endogenous cardioprotective mechanisms through suppression of the VEGF-R2 and Akt-eNOS axis in the heart of mice with type 2 diabetes and subsequently led to cardiac systolic dysfunction resulting from cardiac fibrosis and hypertrophy, which were related to the regression of the microvasculature in the heart. These changes were accompanied by intracardiac hypoxia and oxidative stress. Therefore, the protective role of VEGF appears to be predominantly dependent on its ability to stimulate activation of Akt-eNOS in the endothelial cells in tissues. Further clinical investigations are needed to evaluate whether VEGF inhibition using anti-VEGF agents for the treatment of age-related macular diseases, various cancers, and diabetic microvascular complications has robust effects on the heart, especially in patients with type 2 diabetes.
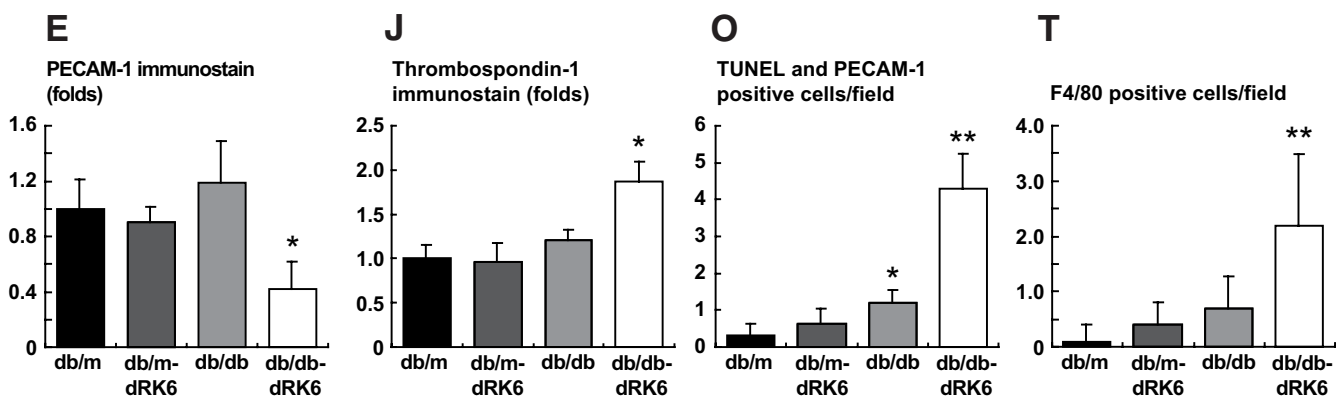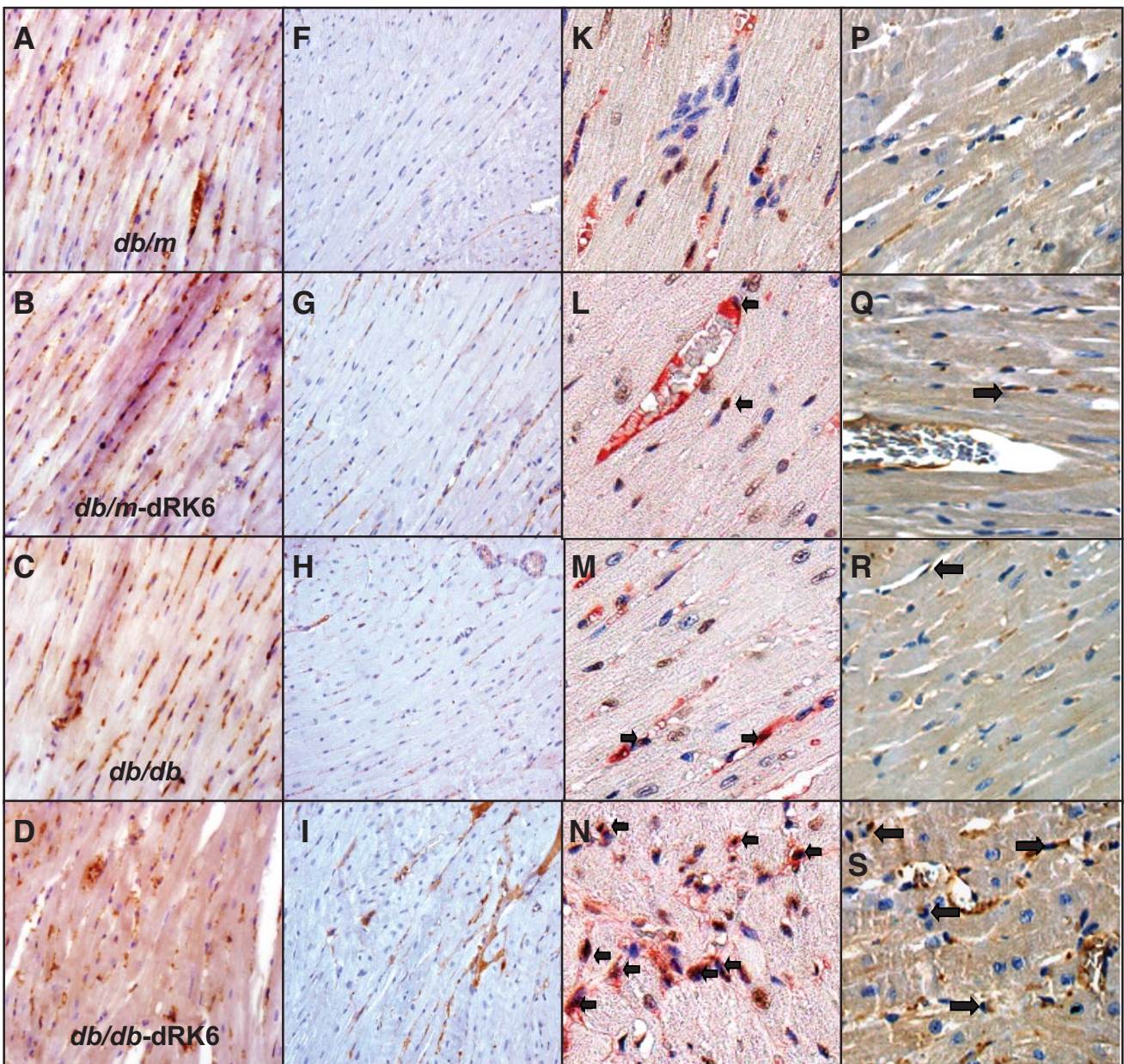
FIG. 5. Myocardial morphology and immunohistochemical staining for PECAM-1, thrombospondin, TUNEL+PECAM-1, and F4/80 in the hearts of diabetic *db/db* and nondiabetic *db/m* mice with or without dRK6 treatment. A representative photomicrograph of myocardial immunostaining for PECAM-1 in nondiabetic *db/m* (*A*), *db/m*-dRK6 (*B*), diabetic *db/db* (*C*), and *db/db*-dRK6 mice (*D*, ×200). Original magnification ×200. Representative immunostains for thrombospondin-1 (*F–I*, ×200), PECAM-1+TUNEL (a dark-brown nuclear for TUNEL-positive and a red cytoplasm for PECAM-1– positive; open arrow, *K–N*, ×400) and F4/80 (open arrow, *P–S*, ×400) in diabetic and nondiabetic *db/db* and *db/m* mice with or without dRK6 treatment. Quantitative assessment of PECAM-1 (*E*), thrombospondin-1 (*J*), PECAM-1+TUNEL (*O*), and F4/80 (*T*) immunoreactivity in diabetic *db/db* and nondiabetic *db/m* mice without or with dRK6 treatment. *$P < 0.05$, **$P < 0.01$ compared with the other groups. (A high-quality color digital representation of this figure is available in the online issue.)
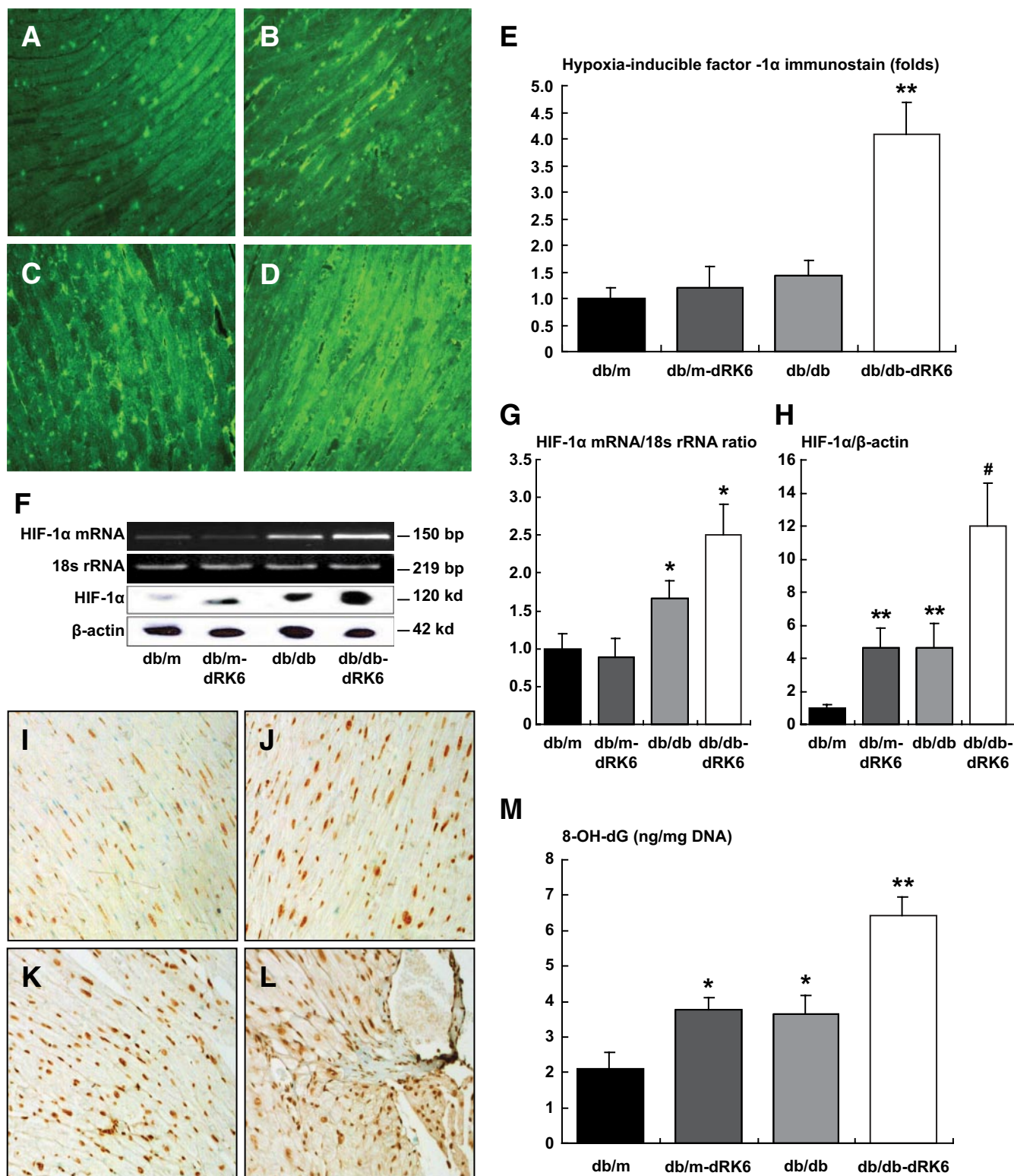
FIG. 6. Immunofluorescent staining for HIF-1α in the heart. Representative pictures illustrating expression in nondiabetic *db/m* (*A*), *db/m*-dRK6 (*B*), diabetic *db/db* (*C*), and *db/db*-dRK6 mice (*D*) in myocytes. Original magnification ×200. *E*: Quantitative assessment of HIF-1α immunoreactivity in the myocardial cells in diabetic *db/db* and nondiabetic *db/m* mice with or without dRK6 treatment. **$P < 0.001$ compared with the other groups. *F*: Expression of HIF-1α protein, mRNA, and 18s rRNA in the hearts of the study groups. Quantitative assessment of the expression of HIF-1α mRNA (*G*) and protein (*H*). *$P < 0.05$, **$P < 0.01$ compared with the other groups, #$P < 0.01$ compared with the *db/db* group; $n = 4$. Immunohistochemical expression of 8-OH-dG protein in myocardial cells. In diabetic *db/db* mice (*K*), 8-OH-dG protein is markedly accentuated in the myocardium (dark nucleus) compared with nondiabetic *db/m* and *db/db*-dRK6 mice (*I* and *J*, respectively). More prominent 8-OH-dG immunostaining is seen in the *db/db*-dRK6 mice compared with the diabetic *db/db* mice (*L*). Original magnification ×200. *M*: Quantitative assessment of 8-OH-dG levels in the DNA from the hearts. *$P < 0.05$, compared with *db/m*, **$P < 0.01$ compared with *db/m* and $P < 0.05$ compared with *db/m*-dRK6 and *db/db*; $n = 4$. (A high-quality color digital representation of this figure is available in the online issue.)
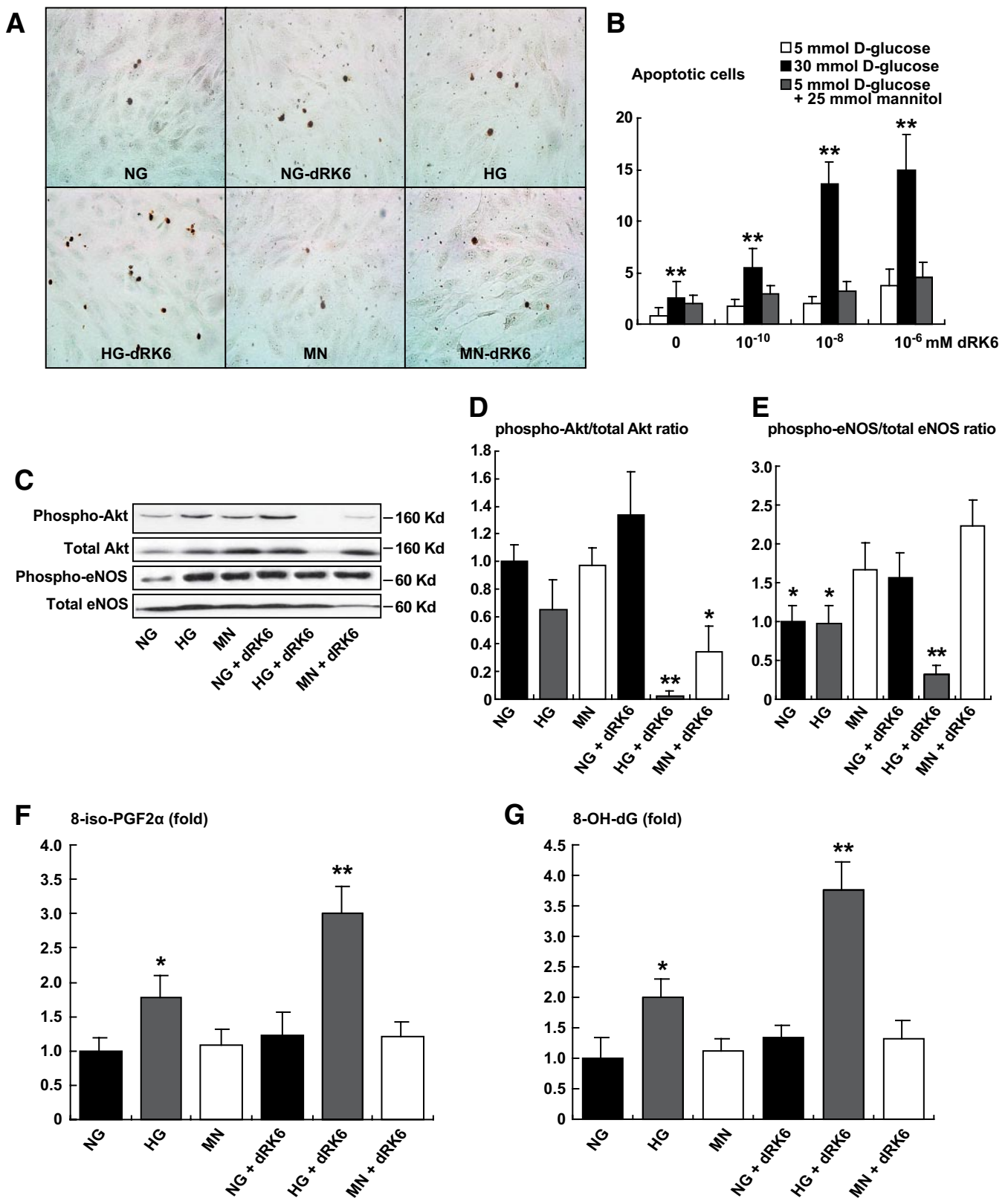
FIG. 7. The effect of dRK6 on apoptosis in the HUVECs, determined by in situ TUNEL assay. Representative pictures of TUNEL-positive HUVECs (*A*, original magnification ×200). The apoptosis of HUVECs treated with different doses of dRK6 (10^{-6}, 10^{-8}, and 10^{-10} mmol/l) and concentrations of glucose in the media (5 and 30 mmol/l of D-glucose, and 5 mmol/l D-glucose + 25 mmol/l mannitol) for 48 h (*B*). Representative Western blots for total and phospho-Akt and phospho-eNOS (*C–E*). 8-Iso-PGF$_{2\alpha}$ (*F*) and 8-OH-dG (*G*) concentrations of cell culture media in each group. *$P < 0.05$, **$P < 0.01$ compared with HG or HG+dRK6. NG, 5 mmol/l of D-glucose; HG, 30 mmol/l D-glucose; MN, 5 mmol/l D-glucose + 25 mmol/l mannitol; +dRK6, treated with dRK6. *$P < 0.05$, **$P < 0.01$ compared with the other groups; $n = 4$. HG, high glucose; NG, normal glucose. (A high-quality color digital representation of this figure is available in the online issue.)

REFERENCES

1. Long R, Sarmiento R, Fanelli M, Capaccetti B, Gattuso D, Gasparini G. Anti-angiogenic therapy: rationale, challenges and clinical studies. Angiogenesis 2002;5:237–256
2. Woodman RJ, Chew GT, Watts GF. Mechanisms, significance and treatment of vascular dysfunction in type 2 diabetes mellitus: focus on lipid-regulating therapy. Drugs 2005;65:31–74
3. Tremolada G, Lattanzio R, Mazzolari G, Zerbini G. The therapeutic potential of VEGF inhibition in diabetic microvascular complications. Am J Cardiovasc Drugs 2007;7:393–298
4. Kamba T, McDonald DM. Mechanisms of adverse effects of anti-VEGF therapy for cancer. Br J Cancer 2007;96:1788–1795
5. Hurwitz H, Saini S. Bevacizumab in the treatment of metastatic colorectal cancer: safety profile and management of adverse events. Semin Oncol 2006;33:S26–S34
6. Picano E. Diabetic cardiomyopathy. The importance of being earliest. J Am Coll Cardiol 2003;42:454–457
7. Adeghate E. Molecular and celluar basis of the aetiology and management of diabetic cardiomyopathy: a short review. Mol Cell Biochem 2004;261:187–191
8. Avogaro A, Vigili de Kreutzenberg S, Negut C, Tiengo A, Scognamiglio R. Diabetic cardiomyopathy: a metabolic perspective. Am J Cardiol 2004;93:13A–16A
9. Poormina IG, Parikh P, Shannon RP. Diabetic cardiomyopathy: the search for unifying hypothesis. Circ Res 2006;98:596–605
10. Fein FS. Diabetic cardiomyopathy. Diabetes Care 1990;13:1169–1179
11. Frustaci A, Kajstura J, Chimenti C, Jakoniuk I, Levi A, Maseri A, Nadal-Ginard B, Anversa P. Myocardial cell death in human diabetes. Circ Res 2000;87:1123–1132
12. Sabbah HN, Sharov VG, Lesch M, Goldstein S. Progression of heart failure: a role for interstitial fibrosis. Mol Cell Biochem 1995;147:29–34
13. Chou E, Suzuma I, Way KJ, Opland D, Clermont AC, Naruse K, Suzuma K, Bowling NL, Vlahos CJ, Aiello LP, King GK. Decreased cardiac expression of vascular endothelial growth factor and its receptors in insulin-resistant and diabetic states: a possible explanation for impaired collateral formation in cardiac tissue. Circulation 2002;105:373–379
14. Miele C, Rochford JJ, Filippa N, Giorghetti-Peraldi S, Van Obberghen E. Insulin and insulin-like growth factor-1 induce vascular endothelial growth factor mRNA expression via different signaling pathways. J Biol Chem 2000;275:21695–21702
15. Yoon YS, Uchida S, Masuo O, Cejna M, Park JS, Gwon HC, Kirchmair R, Bahlman F, Wlater D, Curry C, Hanley A, Isner JM, Losordo DW. Progressive attenuation of myocardial vascular endothelial growth factor expression is a seminal event in diabetic cardiomyopathy: restoration of microvascular homeostasis and recovery of cardiac function in diabetic cardiomyopathy after replenishment of local vascular endothelial growth factor. Circulation 2005;111:2073–2085
16. Jesmin S, Miyauchi T, Goto K, Yamaguchi I. Down-regulated VEGF expression in the diabetic heart is normalized by endothelin ETA receptor antiagonist. Eur J Pharmacol 2006;542:184–185
17. Chiarelli F, Spagnoli A, Bascianin F, Tumini S, Mezetti A, Cipollone F, Cuccurullo F, Morgese G, Verrotti A. Vascular endothelial growth factor in children, adolescents and young adults with type 1 diabetes mellitus: relation to glycaemic control and microvascular complications. Diabet Med 2000;17:650–656
18. Diamant M, Hanemaaijer R, Verheijen JH, Smit JW, Radder JK, Lemkes HH. Elevated matrix metalloproteinase-2 and -9 in urine, but not in serum, are markers of type 1 diabetic nephropathy. Diabet Med 2001;18:423–424
19. Deguchi T, Hashiguchi T, Horinouchi S, Uto T, Oky H, Kimura K, Makisumi K, Arimura K. Serum VEGF increases in diabetic polyneuropathy, particularly in the neurologically active symptomatic stage. Diabet Med 2009;26:247–252
20. Wasada T, Kawahara R, Katsumori K, Naruse M, Omori Y. Plasma concentration of immunoreactive vascular endothelial growth factor and its relation to smoking. Metabolism 1998;47:27–30
21. Blann AD, Belgore FM, McCollum CN, Silverman S, Lip PL, Lip GY. Vascular endothelial growth factor and its receptor, Flt-1, in the plasma of patients with coronary or peripheral atherosclerosis, or type II diabetes. Clin Sci 2002;102:187–194
22. Bae DG, Cho YS, Yoon WH, Chae CB. Arginine-rich anti-vascular endothelial growth factor peptides inhibit tumor growth and metastasis by blocking angiogenesis. J Biol Chem 2000;275:13588–13596
23. Yoo SA, Bae DG, Ryoo JW, Kim HR, Park GS, Cho CS, Chae CB, Kim WU. Arginine-rich anti-vascular endothelial growth factor (anti-VEGF) hexapeptide inhibits collagen-induced arthritis and VEGF-stimulated products of TNF-α and IL-6 by human monocytes. J Immunol 2005;174:5846–1855
24. Semeniuk LM, Kryski AJ, Severson DL. Echocardiographic assessment of cardiac function in diabetic db/db and transgenic db/db-hGLUT4 mice. Am J Physiol Heart Circ Physiol 2002;283:H976–H982
25. Ishizaka N, Saito K, Mitani H, Yamazaki I, Sata M, Usui S, Mori I, Ohno M, Nagai R. Iron overload augments angiotensin II-induced cardiac fibrosis and promotes neointima formation. Circulation 2002;106:1840–1846
26. Baffert F, Le T, Sennino B, Thurston G, Kuo CJ, Hu-Lowe D, McDonald DM. Cellular changes in normal blood capillaries undergoing regression after inhibition of VEGF signaling. Am J Physiol Heart Circ Physiol 2006;290:H547–H559
27. Kamba T, Tam BY, Hashizume H, Haskell A, Sennino B, Mancuso MR, Norberg SM, O'Brien SM, Davis RB, Gowen LC, Anderson KD, Thurston G, Joho S, Springer ML, Kuo CJ, McDonald DM. VEGF-dependent plasticity of fenestrated capillaries in the normal adult microvasculature. Am J Physiol Heart Circ Physiol 2006;290:H560–H576
28. Rivard A, Silver M, Chen D, Keamey M, Magner M, Annex B, Peters K, Isner JM. Rescue of diabetes-related impairment of angiogenesis by intramuscular gene therapy with adeno-VEGF. Am J Pathol 1999;154:355–363
29. Carmeliet P, Ng YS, Nuyens D, Theilmeier G, Brusselmans K, Cornelissen I, Ehler E, Kakkar VV, Stalmans I, Mattot V, Perriard JC, Dowerchin M, Flameng W, Nagy A, Lupu F, Moons L, Collen D, D'Amore PA, Shima DT. Impaired myocardial angiogenesis and ischemic cardiomyopathy in mice lacking the vascular endothelial growth factor isoforms VEGF164 and VEGF188. Nat Med 1999;5:495–502
30. van den Heuvel, van Veldhuisen DJ, van der Wall EE, Blanksma PK, Siebelink HM, Vaalburg WM, van Gilst WH, Crijins HJ. Regional myocardial blood flow reserve impairment and metabolic changes suggesting myocardial ischemia in patients with idiopathic dilated cardiomyopathy. J Am Coll Cardiol 2000;35:19–28
31. Di Mario U, Pugliese G. 15th Golgi lecture: from hyperglycemia to the dysregulation of vascular remodeling in diabetes. Diabetologia 2001;44:674–692
32. Khan ZA, Chakrabarti S. Endothelins in chronic diabetic complications. Can J Physiol Pharmacol 2003;81:622–634
33. Williamson JR, Chang K, Frangos M, Hasan KS, Ido Y, Kawamura T, Nyengaards JR, van den EM, Kilo C, Tilton RG. Hyperglycemic pseudohypoxia and diabetic complications. Diabetes 1993;42:801–813
34. Fang ZY, Prins JB, Marwick TH. Diabetic cardiomyopathy: evidence, mechanisms, and therapeutic implications. Endocr Rev 2004;25:543–567
35. Verma S, Lal BK, Zheng R, Breslin JW, Saito S, Pappas PJ, Hobson RW, 2ND, Duran WN. Hyperglycemia alters phosphatidylinositol 3-kinase (PI3k) and Akt signaling pathways. Am J Physiol Heart Circ Physiol 2005;289:H1744–H1751
36. Murphy E. Primary and secondary signaling pathways in early preconditioning that coverage on the mitochondria to produce cardioprotection. Circ Res 2003;94:7–16
37. Mocanu MM, Yellon DM. PTEN, the Achilles' heel of myocardial ischemia/reperfusion injury? Br J Pharmacol 2007;150:833–838
38. Uchiyama T, Engelman RM, Maulik N, Das DK. Role of AKT signaling in mitochodrial survival pathway triggered by hypoxic preconditioning. Circulation 2004;109:3042–3049
39. Cai Z, Zhong H, Boxch-Marce M, Fox-Talbot K, Wang L, Wei C, Trush MA, Semenza GL. Complete loss of ischaemic preconditioning-induced cardioprotection in mice with partial deficiency of HIF-1α. Cardiovasc Res 2008;77:463–470
40. Semenza GL, Shimoda LA, Prabhakar NR. Regulation of gene expression by HIF-1. Norvatis Found Symp 2006;272:2–8
41. Semenza GL, Jiang BH, Leung SW, Passantino R, Concordet JP, Maire P, Giallongo A. Hypoxia response elements in the aldolase A, enolase 1, and lactate dehydrogenase A gene promoters contain essential binding sites for hypoxia-inducible factor 1. J Biol Chem 1996;271:32529–32537
42. Belke DD, Larsen TS, Gibbs EM, Severson DL. Altered metabolism causes cardiac dysfunction in perfused hearts from diabetic (db/db) mice. Am J Physiol Endocrinol Metab 2000;279:E1104–E1113
43. Barouch LA, Berkowitz DE, Harrison RW, O' Donnell CP, Hare JM. Disruption of leptin signaling contributes to cardiac hypertrophy independently of body weight in mice. Circulation 2003;108:754–759
44. Schrijvers BE, Flyvbjerg A, Vriese SD. The role of vascular endothelial growth factor in renal pathophysiology. Kidney Int 2004;65:2003–2017